Inhibition of Monoamine Oxidase by Pirlindole Analogues: 3D-QSAR and CoMFA Analysis

A. E. Medvedev, A. V. Veselovsky, V. I. Shvedov, O. V. Tikhonova, T. A. Moskvitina,
O. A. Fedotova, L. N. Axenova, N. S. Kamyshanskaya, A. Z. Kirkel, and A. S. Ivanov*,[†]

Laboratory of Biochemistry of Amines and Laboratory of Molecular Graphics Drug Design,
Institute of Biomedical Chemistry, Russian Academy of Medical Sciences, Pogodinskaya Street 10,
Moscow, 119832, Russia

A series of pyrazinocarbazoles, analogues of short acting antidepressant pirlindole (2,3,3a,4,5,6-hexahydro-8-methyl-1*H*-pyrazino[3,2,1-*j,k*]carbazole hydrochloride), were tested as inhibitors of monoamine oxidase A (MAO-A) and B (MAO-B). Rigid analogues exhibited potent and selective inhibition of MAO-A and have size limits (X:Y:Z) of 13.0 × 7.0 × 4.4 Å. Besides MAO-A inhibition flexible analogues also demonstrated potent inhibition of MAO-B and in contrast to rigid analogues their inhibitory activity did not show the dependence on these sizes. The qualitative information (steric and electrostatic coefficients) from the 3D-QSAR with CoMFA models for MAO-A and -B are different, and this information can be used to determine the structural features influencing inhibitor selectivity.

INTRODUCTION

Pirlindole (2,3,3a,4,5,6-hexahydro-8-methyl-1*H*-pyrazino-[3,2,1-*j,k*]carbazole hydrochloride) and its structural analogue, tetrindole (2,3,3a,4,5,6-hexahydro-8-cyclohexyl-1*H*-pyrazino[3,2,1-*j,k*]carbazole hydrochloride) (Figure 1), are effective short acting antidepressants employed clinically.[1−3] They selectively inhibit mitochondrial monoamine oxidase (MAO) type A in vivo and in vitro.[4,5] In both cases MAO inhibition persisted throughout isolation of mitochondria (after in vivo administration) or mitochondria wash (after incubation in vitro),[5−7] typical for such short acting tight-bound MAO-A inhibitors as moclobemide.[8] The development of two antidepressant drugs with very close chemical structure suggests that pyrazinocarbazole is a perspective class for construction of more effective and selective anti-depressants. So the investigation of inhibitory potency of pirlindole analogues possessing various substituents at the eight position (C-8) with subsequent QSAR analysis was the first aim of this study.

Previously we analyzed structure−activity relationship of isatin (indoledione-2,3) (Figure 1) derivatives as MAO inhibitors.[9] They are competitive and reversible MAO inhibitors, possessing relatively rigid structures. Most of isatin analogues have planar structures and the length and width of most potent MAO-A inhibitors did not exceed 14.0 and 6.0 Å, respectively, whereas selective MAO-B inhibitors had smaller sizes (8.5 and 5.0 Å, respectively).[9] Some isatin analogues possessing 3D structure with "thickness" of molecule not more than 4.5 Å demonstrated more potent MAO-A inhibition, than isatin. If size of molecules, which competitively interact with either type of MAO, actually reflects some properties of active site volume of these enzymes, we could expect that compounds from other chemical classes acting in a similar manner must demonstrate similar depen-
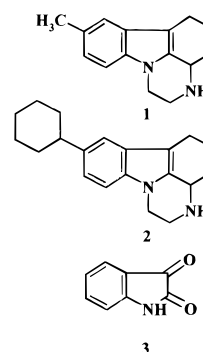

Figure 1. 2D-structures of basic compounds used in our QSAR studies. 1 − pirlindole, 2 − tetrindole, 3 − isatin.

dence between 3D sizes and inhibitory activity. That data were submitted to a three-dimensional QSAR (3D-QSAR) approach using comparative molecular field analysis (CoMFA).[10] The CoMFA model gave good prediction not only for MAO inhibitory activity of our compounds but also for isatin analogues tested in the other laboratory.[11] So the investigation of applicability of previously developed models for MAO inhibitors from another chemical class of compounds was the second aim of this study.

Data of the present report provide further evidence indicating volume differences of active sites of MAO-A and -B. CoMFA models for MAO-A and -B are also different, and this is a good basis for determination of structural features required for chemical compounds which are developed as selective MAO-A or -B inhibitors.

MATERIALS AND METHODS

Chemicals. Pirlindole and its analogues were synthesized as described previously.[1,12−17] ^{14}C-Labeled 5-hydroxy[side chain 2-^{14}C]tryptamine creatinine sulfate (5HT) and 2-phen-yl[1-^{14}C] ethylamine HCl (PEA) were obtained from Ra-
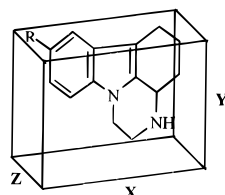
[†] E-mail: ivanov@ibmh.msk.su. Fax: 07-(095)-245-0857.

Figure 2. Minimal box dimensions for determination of linear sizes of pirlindole analogues.
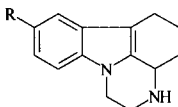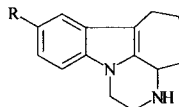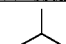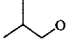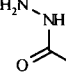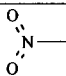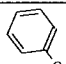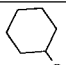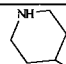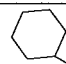
diochemical Centre (Amersham, UK). Cold amines were purchased from Sigma Chemical Co. (St. Louis, MO). Other chemicals of highest grade available were produced by Reakhim (Moscow, Russia).

Determination of MAO Activity and Its Inhibition. Rat liver mitochondria were used as a source of MAO-A and MAO-B. The activity of MAO was assayed radiometrically[18] with minor modifications[5] using 0.1 mM [^{14}C]-5-hydroxy-tryptamine (serotonin) and 5 μM [^{14}C]-phenylethylamine as substrates for MAO-A and -B, respectively. These concen-

trations which are either close to or below K_m value allow competitive inhibition to be detected. To obtain reliable comparative IC$_{50}$ values (concentration required for 50% inhibition of enzymatic activity) rat liver mitochondria were incubated at 37 °C for 30 min with all suspected MAO inhibitors, and the enzymatic activity was measured thereafter by adding substrates of MAO-A and -B. Such approach is widely used for pilot studies of potential MAO inhibitors.[19] Time-dependence of MAO-A inhibition was investigated using initial concentrations of the inhibitors near IC$_{50}$ values obtained in the above-described experiments.

Computer Modeling. Most of the calculations were carried out on Silicon Graphics Workstation Indigo-2 (R4400, XZ) using Sybyl 6.3 software (Tripos Inc., U.S.A.). The molecular models were constructed, and t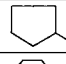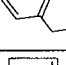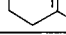heir geometries were optimized using the standard Tripos force field. The atomic charges calculation and geometry optimization of molecules were made by semiempirical AM1 method. They were used in the subsequent analysis. Values of molecular

Table 1. Inhibitory Activity (IC$_{50}$, μM) and Size (Å) of Pirlindole Analogues

| Name | R | MAO-A | | MAO-B | | Size | | |
		Exp.	Pred.	Exp.	Pred.	X	Y	Z
P1		0.11	0.11	>>100	97.7	10.894	6.959	4.355
P2		0.04	0.04	20	19.1	13.462	7.031	3.498
P3		12.6	13.0	>178	182	11.433	7.121	2.854
P4	F—	3.98	3.80	>178	182	8.791	6.912	2.829
P5	H$_3$C—	0.071	0.08	158	182	9.746	6.909	2.828
P6		7.9	8.13	250	245	9.871	7.027	2.849
P7		0.79	0.83	180	174	12.991	7.198	4.448
P8	H$_2$N—	4.0	3.80	>1000	912	9.532	6.894	2.827
P9		13.0	13.18	16.0	15.5	12.704	7.089	3.521
P10		0.26	0.24	12.5	11.75	13.286	6.829	4.151
P11		0.5	0.51	>500	525	11.784	6.969	4.006
P12		0.53	0.5	29.0	30.2	13.051	7.019	4.393
P13		0.08	0.07	160	160	12.340	7.043	4.360
P14		0.13	0.14	7.5	7.5	13.002	7.064	2.869
P15		0.14	0.13	0.14	0.14	14.944	7.093	2.869
P16		0.03	0.03	79.4	79.4	12.070	7.096	3.031

hydrophobicity were calculated by method of Moriguchi et al.[20] Linear sizes of pirlindole and its derivatives were calculated using HyperChem 4.5 software (Hypercube Inc., Canada) by constructing boxes around molecules. Sizes of minimal box in which given compound fits were considered as sizes of the molecule. Simple geometrical dimensions (X:Y:Z) of each molecular model were measured as shown in Figure 2. Conformational analysis was done using Random search program of Sybyl.

For 3D-QSAR with CoMFA analysis[21] the inhibitors were aligned by fitting indole part of molecules structure atom by atom. The region was generated automatically by the program. The grid size had a resolution of 2 Å. Both steric and electrostatic fields were taken into consideration. The steric and electrostatic potentials were generated using a sp^3 carbon probe and a $+1$ charge. QSAR analysis was carried out in two steps using PLS technique. In the first analysis, using five components and a number of cross-validation groups equal to a number of compounds, the optimal number of components was determined. The optimal number of components for the final 3D-QSAR model was chosen as the number of components that corresponds to the minimum cross-validated standard error of estimate (s_{cv}) and $r^2_{cv} >$ 0.4. The second run was performed without cross-validation, using the optimal number of components previously determined. The results of the second analysis were used for drawing the coefficients' contour maps.

RESULTS

In accordance with previous studies[4,5] pirlindole selectively inhibited MAO-A (see Table 1). With the exception of compounds P9 and P15 all other analogues also exhibited selective inhibition of MAO-A. Values of IC$_{50}$ varied for MAO-A from 0.03 (μM (compound P16) to 13 μM (compound P9), suggesting the essential role of substituents at C-8 for manifestation of MAO inhibition. Study of the dependence of MAO-A inhibition on preincubation time with the compounds revealed that they could be divided into two groups. Compounds of the first group exhibited properties of time-dependent MAO-A inhibitors, whereas compounds of the second group did not demonstrate this property (Figure 3). These data suggest that the nature of substituents at C-8 stipulates property of time-dependent inhibition. However, the elucidation of a possible interrelationship between chemical structure of substituents at C-8 and manifestation of the time-dependent inhibition requires further investigation.

We have initially determined molecular sizes of pirlindole analogues (Table 1). Molecular sizes of pyrazinocarbazole nucleus are within limits found for isatin analogues, exhibiting potent inhibition of either MAO. At the first sight, comparison of molecular sizes and the inhibitory activity did not reveal any dependence between these parameters (Table 1, Figure 4). However, the rigid pirlindole analogues demonstrated most selective inhibition of MAO-A versus MAO-B (see P1, P3−P8, P11−P14, P16). The sizes of most potent MAO-A inhibitors have the following limits: 13.0 × 7.1 × 4.5 Å. Flexible analogues possessing more rotation points than in rigid compounds were also potent inhibitors of MAO-A. However, they exhibited potent MAO-B inhibition as well. The inhibitory effect of compound P15 was equipotent with respect to both MAO. These observations
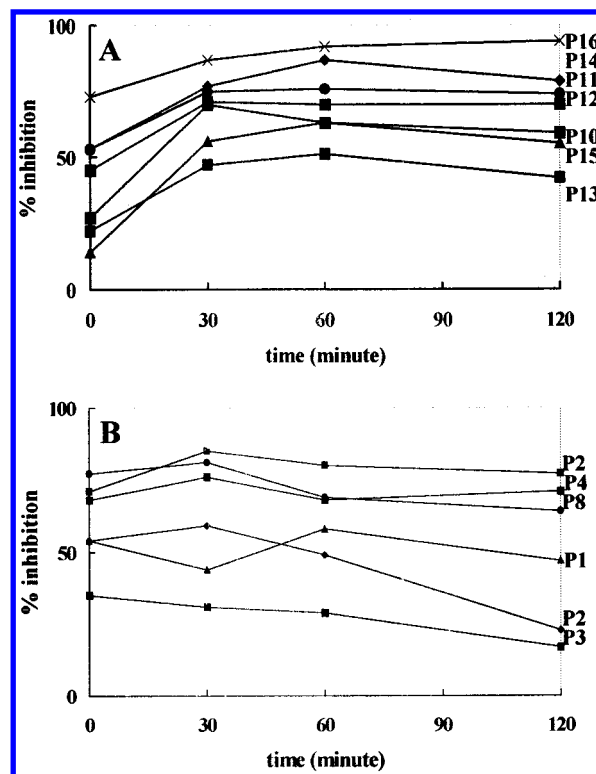
Figure 3. Time-course of MAO-A Inhibition by pirlindole analogues. A − compounds that show time-dependent inhibition. B − compounds that do not show time-dependent inhibition. Other details are given in the Material and Methods section.
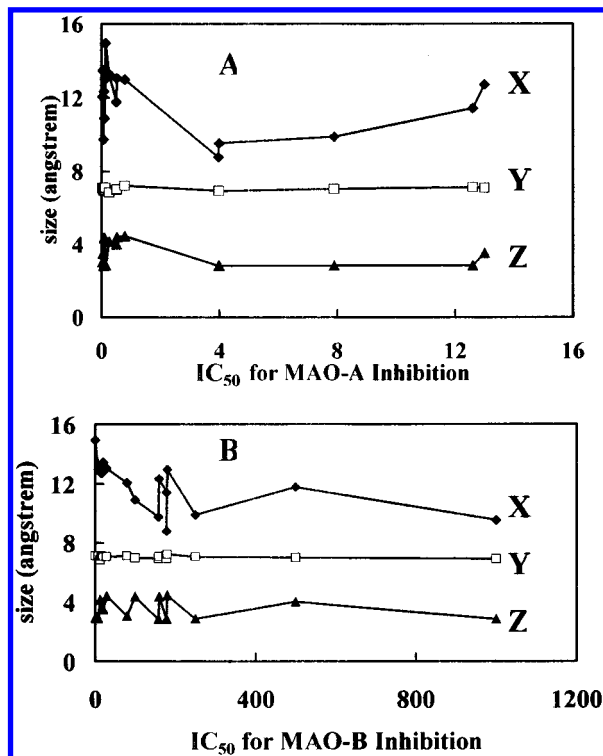
Figure 4. Relationship between the sizes of pirlindole analogues and their inhibitory activity (μM). A − MAO-A; B − MAO-B. All symbols indicate pirlindole analogues.

support our hypothesis that relatively rigid and selective inhibitors of MAO-A possess larger size substituents along the *X*-axis.

To help confirm our hypothesis and elucidate the structural features influencing inhibition and selectivity we developed

Figure 5. Standard dev*coefficients contour plot of CoMFA fields of MAO-A. A. Steric fields. Sterically disfavored areas (contribution level of 30%) are represented by solid lines; sterically favored areas (contribution level of 70%) − by dashed lines. B. Electrostatic fields. Positive charge favored areas (contribution level of 80%) are represented by solid lines; negative charge favored areas (contribution level of 20%) − by dashed lines.

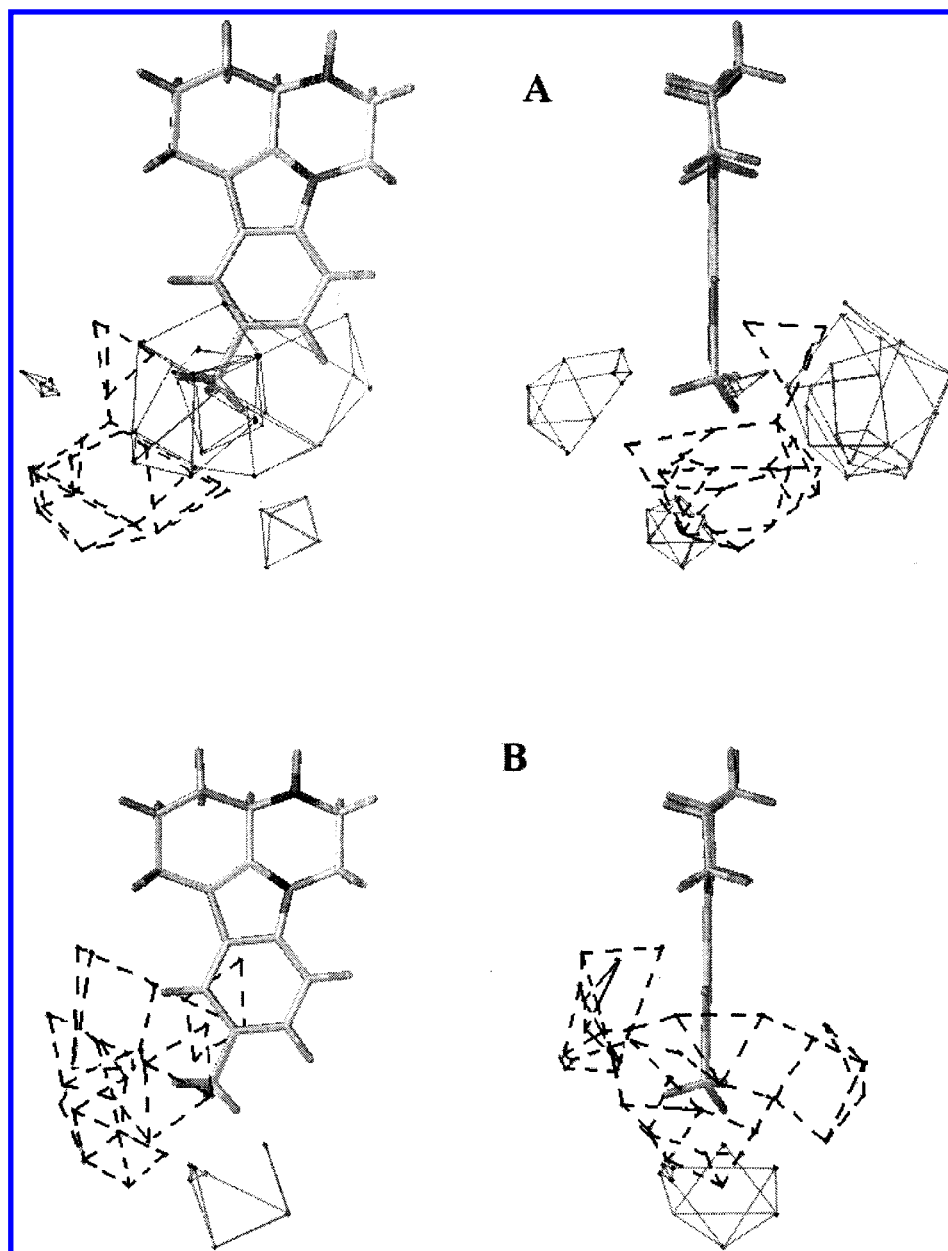several 3D-QSAR with CoMFA models from pirlindole analogues. Most of these compounds have rigid structures. Only three of them have the flexible substituents (p2, p3, and p15), and the conformer analysis was initially done for these flexible molecules. This analysis showed that the conformers of these compounds could be divided into two groups: the stretch "long" conformers and the "short" conformers with the turn of the substituents (view of these conformations for the inhibitor p2 is shown at Figure 7). The attempts to design the model for MAO-A with 16 inhibitors using only long or only short conformers for flexible compounds in analysis were not successful. The model was designed using the compounds p2 and p3 in the long conformation and p15 (molecule with the longest substituent) in the short conformation. The model for MAO-B was designed using the same conformation of inhibitors. The quantitative results of this QSAR analysis

are summarized in Table 2. The obtained models were statistically significant and had a good predictive power for the test molecules. More reliable model for MAO-B was constructed using the hydrophobic values (logP) of inhibitors (Table 2), whereas this parameter was not important for MAO-A inhibition. This is in accordance with data from the other laboratory.[22] For MAO-A model the relative contributions of the independent variables show that the distribution of steric and electrostatic fields are the equal. Steric fields of the compounds have a major contribution in determining MAO-B inhibitory activity. This is also consistent with our hypothesis that molecular sizes of rigid pirlindole analogues can provide predictable manifestation of MAO-B inhibition.

Such models can explain more than 90% of the inhibitory potency of the compounds with respect to both enzymes. The models also have good predictive ability: cross-validated
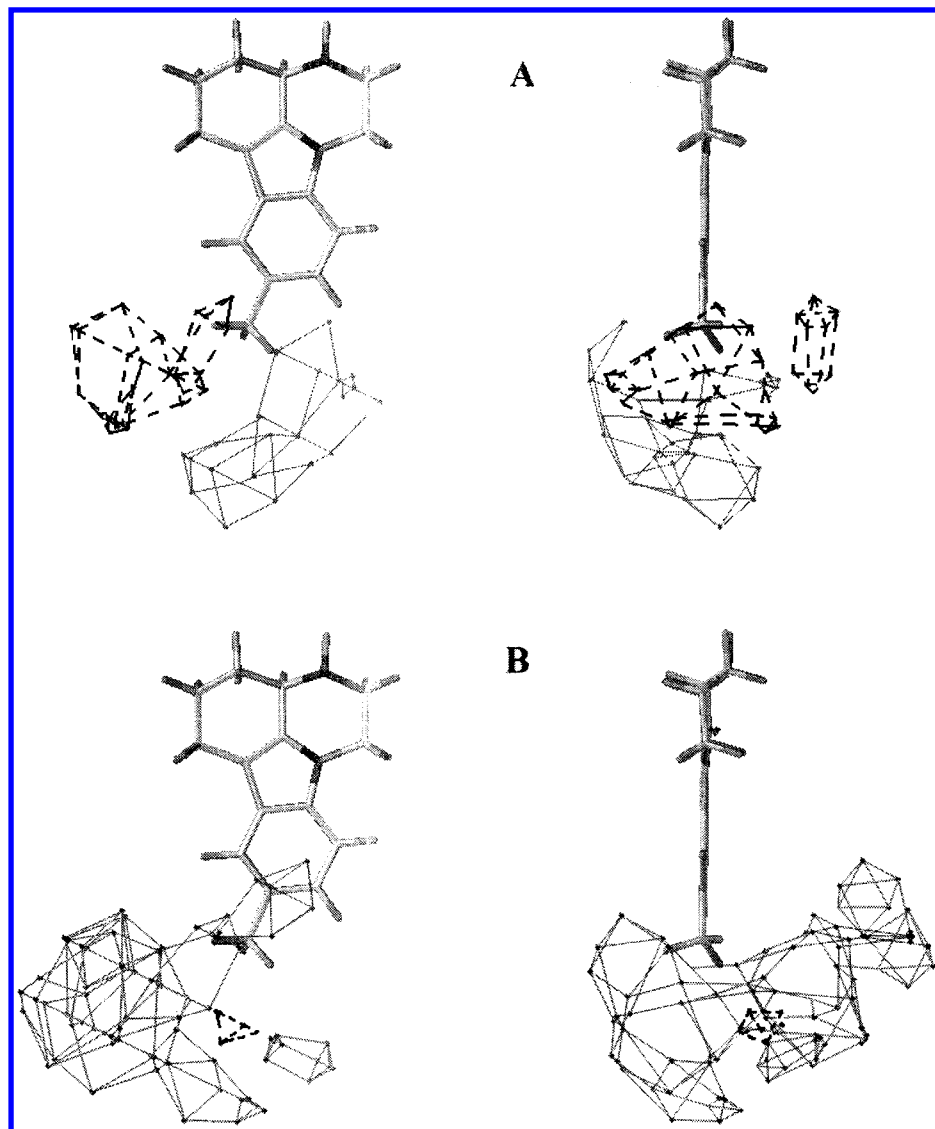
Figure 6. Standard dev*coefficients contour plot of CoMFA fields of MAO-B. A. Steric fields Sterically disfavored areas (contribution level of 30%) are represented by solid lines; sterically favored areas (contribution level of 70%) − by dashed lines. B. Electrostatic fields. Positive charge favored areas (contribution level of 80%) are represented by solid lines; negative charge favored areas (contribution level of 20%) − by dashed lines.
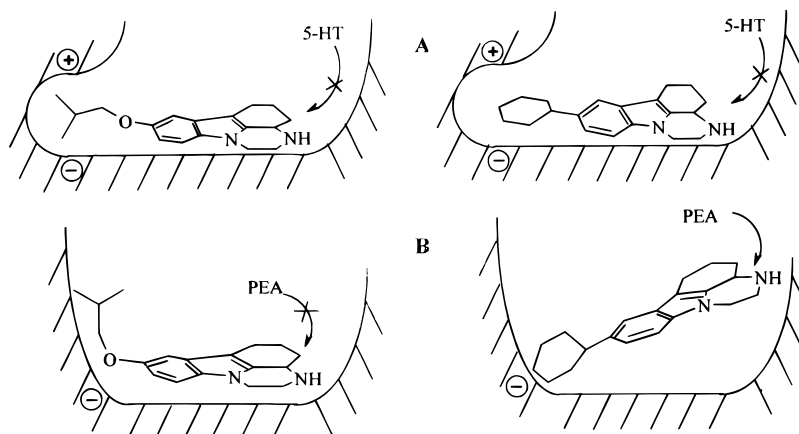
Figure 7. Schemes of MAO-A (A) and MAO-B (B) active site structures and putative positions of P2 (left) and tetrindole (right) molecules. Arrows show that phenylethylamine (PEA) can displace tetrindole, but not P2. Serotonin (5-HT) cannot displace both molecules.

r^2 values were 0.444 and 0.468 for MAO-A and MAO-B, respectively (Table 2). For further examination of the predictive property of our models we compared predicted values of IC_{50} for MAO inhibition by tetrindole with the experimental data (Table 3). The search for stable conformations around the bond between pyrazinocarbazole nucleus and cyclohexane of tetrindole showed that molecule has two stable conformers with the same energy. Prediction of these

Table 2. 3D-QSAR with CoMFA Analysis for MAO-A and MAO-B[a]

	MAO-A						MAO-B					
	r^2_{cv}	s_{cv}	n	r^2	s	F	r^2_{cv}	s_{cv}	n	r^2	s	F
3D QSAR + CoMFA	0.444	0.83	5	0.97	0.19	65	0.525	0.56	4	0.98	0.15	131
steric fields				50%						62%		
electrostatic fields				50%						38%		
3D QSAR + CoMFA + logP	0.300	0.89	4				0.625	0.45	3	0.91	0.22	34
steric fields										49%		
electrostatic fields										21%		
logP										30%		

[a] r^2_{cv} − square of the multiple correlation coefficients in analysis with cross-validation, s_{cv} − cross-validated standard error of estimate, n − optimal number of components, r^2 − square of the multiple correlation coefficients without cross-validation, s − standard error, F − significance test, logP − logarithm of partition coefficient in octanol/water system.

Table 3. Values of Experimental and Predicted Inhibitory Activity of Tetrindole for MAO-A and -B[a]

Enzyme	Tetrindole inhibitory activity (IC$_{50}$, M)		
	experiment	Conformer 1	Conformer 2
MAO-A	4.5×10^{-8}	13.5×10^{-8}	33.1×10^{-8}
MAO-B	6.3×10^{-5}	1.8×10^{-5}	19.5×10^{-5}

[a] The values of experimental activity from Medvedev et al.[5]

inhibitory activity shows that the higher predicted values from two conformers are in a good agreement with experimental values determined earlier.[5] So, our models satisfactorily describe the inhibitory properties of pyrazinocarbazole analogues.

The three-dimensional steric and electrostatic contour maps were analyzed from these models. Figure 5 shows the important steric (A) and electrostatic (B) regions influencing MAO-A inhibition. Pirlindole was added as a reference to better visualize the location of these regions. Favorable steric fields can be seen along the *X*-axis where substituents with increased length demonstrated enhanced inhibition. Unfavorable steric regions can be seen on either side of substituents. The QSAR model used two electrostatic regions to explain part of the variation in MAO-A inhibition. The favorable region for negative charges is localized at the same places as the favorable steric regions, and the other favorable region for positive charges is located at adjacent site in the plane of pyrazinocarbazole nucleus (see Figure 5).

The distribution of steric and electrostatic coefficients in the MAO-B 3D-QSAR with CoMFA model differed considerably from the distribution of coefficients in the MAO-A model. An unfavorable steric field limits the length of C-8 substituents in the MAO-B model, while a favorable steric region can be seen at an adjacent site (Figure 6). The electrostatic coefficients in the MAO-B model identify two favorable regions for positive charge near the substituent site.

Thus, the comparison of 3D-QSAR models of MAO-A and -B inhibition developed a series of pirlindole analogues

revealed significant differences in steric and electrostatic fields. The qualitative structural information from these models suggests an underlying reason for the different inhibitor selectivity between MAO-A and -B.

DISCUSSION

Previously we analyzed isatin analogues as inhibitors of MAO-A and -B.[9] They were readily reversible competitive inhibitors of either MAO. Within this group of compounds the selective inhibitors of MAO-A and -B had different volume sizes. 3D-QSAR + CoMFA analysis confirmed this conclusion and revealed certain regions in these compounds essential for manifestation of selective inhibition of MAO-A and -B.[10] The constructed models successfully described not only our own data but also results obtained in the other laboratory.[11]

In the present report we have investigated possible applicability of that models for the inhibitors from the other chemical class. In contrast to isatin pirlindole and its analogues exhibited properties of tight-bound inhibitors.[7] It is still unclear whether pirlindole undergoes MAO-dependent (time-dependent) redox-conversion in vivo.[23] So, the mechanism of MAO inhibition by pirlindole completely differs from that of isatin, and consequently, a previously developed model required validation using the other type of MAO inhibitors.

Evaluation of 3D sizes of pirlindole analogues revealed that the length sizes of rigid compounds exhibiting potent

and selective inhibition of MAO-A are within limits previously determined for isatin analogues, selective inhibitors of MAO-A. However, we should emphasize that all isatin analogues have sizes along the *Y*-axis of 5.0−6.0 Å, whereas these sizes in most pirlindole analogues were a bit larger (6.9−7.2). Some isatin analogues possessing 3D structure with "thickness" of molecule not more than 4.5 Å (size along *Z*-axis) also demonstrated more potent MAO-A inhibition than isatin.[9] This is in accordance with the present data.

In contrast to rigid compounds, flexible pirlindole analogues possessing substituents at C-8 with rotation points did not demonstrate such dependence between sizes of molecules and the inhibitory activity. The most probable explanation of these discrepancies consists of differences of binding sites for pirlindole analogues in MAO-A and MAO-B molecules. The active site of MAO-A has enough space to accommodate rather long rigid inhibitors (Figure 7). It is possible that the geometry of MAO-B active site is more complex, and long rigid molecules cannot be accommodated in it. If this suggestion is correct, an increase in the MAO-B inhibitory activity of flexible analogues can be explained by the possibility of such conformation that corresponds to the geometry of the active site of MAO-B. Many inhibitors of MAO-B are flexible compounds, and a limitation in flexibility of molecules often decreases MAO-B inhibitory activity. For example, long and flexible oxodiazolones are very potent inhibitors of MAO-B, whereas shorter but rigid analogues are less potent.[24]

Our 3D-QSAR + CoMFA models for MAO-A and -B provide further evidence for steric differences of the active sites of these enzymes. Comparison of steric fields of pirlindole analogues as MAO-A and MAO-B inhibitors suggests the existence of steric obstacle at C-8 (Figure 6) in MAO-B molecule, which might explain inability of long rigid pirlindole analogues to be potent inhibitors of MAO-B. For MAO-A inhibitors increase of the length of molecule in this region potentates their activity. This generally agrees with our previous studies on isatin analogues.[9,10] Also 3D-QSAR + CoMFA suggests that MAO-A inhibition requires certain limits in the size of substituents, so that "width" of the (rigid) molecule be less than 4.5 Å (see Table 1). Such distribution of steric fields suggests that the active site of MAO-A might represent a relatively narrow slot, whereas the active site of MAO-B is shorter but wider. Comparison of steric and electrostatic fields of these models revealed that regions of positive and negative charges are near the favorable steric region. It is possible that charged amino acid residues of MAO-A form a cavity accommodating substituents of pirlindole analogues. Distribution of the fields for MAO-B suggests that negatively charged amino acid residues in the active site of MAO-B probably determine limitation of the length of substituents at C-8. Electrostatic fields of MAO-B model are characterized by the existence of favorable regions for positive charges, whereas these places in MAO-A model require negative charge. Also MAO-B model takes into consideration hydrophobicity of compounds employed. This is in accordance with the general notion that preferential substrates and selective inhibitors of MAO-B are more hydrophobic compounds than that of MAO-A.[22,25] Our conclusion does not contradict with the latest data of mutation analysis.[26] A single mutation in which Phe-208 in MAO-A was substituted for relatively more hydrophobic Ile (corresponding residue in MAO-B primary structure) resulted in dramatic alteration in the sensitivity to diagnostic acetylenic inhibitors chlorgyline and deprenyl and to a lesser extent in appearance of some substrate specificity typical for MAO-B.

It is necessary to emphasize that either type of MAO can probably interact with a certain conformer of inhibitor. For example, tetrindole can exist in two preferential conformations characterized by the same energy level. Prediction of MAO-A inhibition by the conformer 1 is close to the experimental values. A better coincidence of predicted inhibition of MAO-B with experimental data is observed for conformer 2 (see Table 3). So it is possible that experimentally observed values reflect interaction of MAO-A and -B with certain tetrindole conformer, which is preferential for the given enzyme (MAO-A or MAO-B).

Thus, using pirlindole analogues as inhibitors of MAO-A and MAO-B we have developed significant 3D-QSAR + CoMFA models of active sites of these enzymes. The models revealed spatial differences in the active sites of both enzymes. Data of the present report can be used for the design of new generation of selective reversible inhibitors of MAO.

REFERENCES AND NOTES

(1) Mashkovsky, M. D.; Grinev, A. N.; Andreeva, N. I.; Altukhova, L. B.; Shvedov, V. I.; Avrutsky, G. Ya.; Gromova, V. V. New Antidepressive Preparation Pyrazidole. *Khim. Pharm. Zh.* **1974**, *8*, 60−63 (in Russian).
(2) Mashkovsky, M. D. *Drug Reference Book*, Meditzina Moscow, 1993 (in Russian).
(3) Bruhwyler, J.; Liegeois, J. F.; Geczy, J. Pirlindole: A Selective Reversible Inhibitor of Monoamine Oxidase A. A Review of Its Preclinical Properties. *Pharmacol. Res.* **1997**, *36*, 23−33.
(4) Gorkin, V. Z. Studies on the Nature and Specific Inhibition of Monoamine Oxidases. In *Neuropharmacology* '85; Kelemen, K.; Magyar, K.; Vizi, E. S., Eds.; Akademiai Kiado: Budapest, 1985; pp 9−14.
(5) Medvedev, A. E.; Kirkel, A. Z.; Kamyshanskaya, N. S.; Moskvitina, T. A.; Axenova, L. N.; Gorkin, V. Z.; Andreeva, N. I.; Golovina, S. M.; Mashkovsky, M. D. Monoamine Oxidase Inhibition by Novel Antidepressant Tetrindole. *Biochem. Pharmacol.* **1994**, *47*, 303−308.
(6) Medvedev, A. E.; Gorkin, V.; Shvedov, V.; Fedotova, O.; Fedotova, I.; Semiokhina, A. Efficacy of Pirlindole, a Highly Selective Reversible Inhibitor of Monoamine Oxidase Type A, in the Prevention of Experimentally Induced Epileptic Seizures. *Drug Investigation* **1992**, *4*, 501−507.
(7) Medvedev, A. E.; Shvedov, V. I.; Chulkova, T. M.; Fedotova, O. A.; Saedereup, E.; Squires, R. Effects of the Antidepressant Pirlindole and its Dehydro-derivative on the Activity of Monoamine Oxidase-A and on GABA-A Receptors. *Neurochem. Res.* **1996**, *21*, 1519−1524.
(8) Keller, H. H.; Kettler, R.; Keller, G.; Da Prada, M. Short-acting Novel MAO Inhibitors: in vivo Evidence for the Reversibility of MAO Inhibition by Moclobemide and Ro 16−6491, Naunyn Schmiedebergs. *Arch. Pharmacol.* **1987**, *335*, 12−20.
(9) Medvedev, A. E.; Ivanov, A. S.; Kamyshanskaya, N. S.; Kirkel, A. Z.; Moskvitina, T. A.; Gorkin, V. Z.; Li, N. Y.; Marshakov, V. Yu. Interaction of Indole Derivatives with Monoamine Oxidase A and B. Studies on the Structure-inhibitory Activity Relationship. *Biochem. Mol Biol. Int.* **1995**, *36*, 113−122.
(10) Medvedev, A. E.; Ivanov, A. S.; Veselovsky, A. V.; Skvortsov, V. S.; Archakov A. I. QSAR Analysis of Indole Analogues as Monoamine Oxidase Inhibitors. *J. Chem. Inf. Comput. Sci.* **1996**, *36*, 664−671.

(11) Rajesh, K.; Romesh, C. B.; Mahmood, A.; Parvez, S. H. Inhibition of Rat Brain Monoamine Oxidase by Isatin and its Structural Analogues. *Biogenic Amines* **1994**, *10*, 473−485.

(12) Shvedov, V. I.; Altukhova, L. B.; Grinev, A. N. Synthesis of 1,10-trimethylenepyrazino[1,2-a]indoles. *Khim. Pharm. Zh.* **1967**, *1(3)*, 25−30 (in Russian).

(13) Shvedov, V. I.; Fedorova, I. N.; Nirkova, V. G., Volschina, O. N.; Kunoverov, V. V. Synthetic Method for 5,6-dihydro-8-methyl-(cyclohexil)-4*H*- pyrazino[3,2,1-*j,k*]carbazole Hydrochloride. *USSR author's sertificate N 1.235.183*.

(14) Shvedov, V. I.; Altukhova, L. B.; Grinev, A. N. Synthetic Method for 5,6-trimethylen-2,3,4,5-tetrahydro-γ-isocarboline. *USSR author's certificate N 194.827. Byull. Isobret.* **1967**, *9*, 45.

(15) Dvoryantseva, G. G.; Pol'shakov, V. I.; Sheikner, Yu. N.; Shvedov, V. I.; Grinev, A. N.; Mashkovsky, M. D.; Karapetyan, H. A.; Strukov Y. T. Structure−activity Relationship in Pyrazino[3,2,1-*j,k*]carbazole Derivatives. *Eur. J. Med. Chem.-Chem. Ther.* **1985**, *230*, 414−418.

(16) Shvedov, V. I.; Mashkovsky, M. D.; Savitskaya, N. V.; Andreeva, N. I.; Fedorova, I. N. 2,3,3a,4,5, 6-Hexahydro-8-cyclohexil-1*H*-pyrazino-[3,2,1-*j,k*]carbazole Hydrochloride with Psychotropic Action. *USSR author's certificate N, Byull. Isobret.* **1991**, *44*.

(17) Medvedeva, M. V.; Fedotova, O. A.; Shvedov, V. I.; Belov, A. A.; Medvedev, A. E.; Bobruskin, I. D. Action of Antidepressant Pirlindole and Its Nitroanalogue on cGMP-dependent Cyclic Nucleiotide Phosphodiesterase from Soluble Fraction of Human Brain Cortex. *Biochemistry (Moscow).* **1993**, *58*, 789−798 (in Russian).

(18) Tipton, K. F.; Youdim, M. B. H. Assay of Monoamine Oxidase. In *Monoamine Oxidase and its Inhibition*; Wolstenholm, G. E. W., Knight, J., Eds.; Elsevier: Amsterdam, 1976; pp 393−403.

(19) Da Prada, M.; Kettler, R.; Keller, H. H.; Burkland, W. P.; Haefely, W. E. Preclinical Profiles of the Novel Reversible MAO-A Inhibitors, Moclobemide and Brofaromine, in Comparison with Irreversible MAO Inhibitors. *J. Neural Transm.* **1989**, *28(Suppl)*, 5−20.

(20) Moriguchi, I.; Hirono, S.; Nakagome, I. Comparison of Reliability of logP Values for Drugs Calculated by Several Methods. *Chem. Pharm. Bull.* **1994**, *42*, 976−978.

(21) Cramer, R. D. III; Petterson, D. E.; Bunce, J. D. Comparative molecular field analysis (CoMFA). 1. Effect of share on binding of steroids to carrier proteins. *J. Am. Chem. Soc.* **1988**, *110*, 5959−5967.

(22) Altomare, C.; Carrupt, P.-A.; Gaillard, P.; Tayar, N. E.; Testa, B.; Carotti, A. Quantitative Structure-Metabolism Relationship Analyses of MAO-Mediated Toxication of 1-Methyl-4-phenyl-1,2,3,6-tetrahydropyridine and Analogues. *Chem. Res. Toxicol.* **1992**, *5*, 366−375.

(23) Baumanis, E. A.; Birska, I. A.; Reikhman, G. O.; Shvedov, V. I.; Gorkin, V. Z. On the Mechanisms of Modification by Pyrazidole of the Catalytic Activity of Mitochondrial Monoamine Oxidase. *Vopr. Med. Khim. (Moscow)* **1987**, *6*, 90−96.

(24) Kruger, M. J.; Mazouz, F.; Ramsay, R. R.; Milcent, R.; Singer, T. P. Dramatic Species Differences in the Susceptibility of Monoamine Oxidase B to a Group of Powerful Inhibitors. *Biochem. Biophys. Res. Com.* **1995**, *206*, 556−562.

(25) Thull, U.; Kneubuhler, S.; Gaillard, P.; Carrupt, P.-A.; Testa, B.; Altomare, C.; Carotti, A.; Jenner, P.; McNaught, K. S. P. Inhibition of Monoamine Oxidase by Isoquinoline Derivatives. Qualitative and 3D-quantitative Structure−activity Relationships. *Biochem. Pharmacol.* **1995**, *50*, 869−877.

(26) Tsugeno, Y.; Ito, A. A Key Amino Acid Responsible for Substrate Selectivity of Monoamine Oxidase A and B. *J. Biol. Chem.* **1997**, *272*, 14033−14036.